CDF note 9712

Search For Single Top Quark Production Optimized for s-channel Production with 3.2 fb^{-1} Data

The CDF Collaboration
URL http://www-cdf.fnal.gov
(Dated: February 28, 2009)

This note describe an updated result of s-channel-optimized search for single top quark production using 3.2 fb^{-1} of data accumulated with the CDF detector. From the previous result with 2.7 fb^{-1}, we additionally used 500 pb^{-1} of new data and applied a cut to suppress QCD background event. As a result, we found that the probability (p-value) that the candidate events originate from a background fluctuation in the absence of single top s-channel production is 0.022, which is equivalent to 2.01σ deviations in Gaussian statistics, and this excess corresponds to the single top s-channel cross section of $1.49^{+0.92}_{-0.75}$ pb. An observed value of $|V_{tb}|$ is $1.32^{+0.27}_{-0.26}$(experimental) $\pm\, 0.10$(theory). We also set the 95 % CL. upper limit of $\sigma_s = 3.49$ pb for the s-channel production cross section.

Preliminary Results for Winter 2009 Conferences

I. INTRODUCTION

Top quarks are predominantly produced in pairs via the strong interaction, in $\bar{p}p$ collisions at Tevatron with $\sqrt{s}=$ 1.96 TeV. Top quark has a weak isospin 1/2 composing a weak isospin doublet with a bottom quark. It predict not only top quark pair production via strong interaction but also singly produced together with a bottom quark via weak interaction. However, finding single top quark production is challenging since it is rarely produced($\sigma_{\rm singletop}$=2.9 pb [1]) against background processes with the same final state like W+jets and $t\bar{t}$. Since the signal to background ratio is small, The mesurement of electroweak single top production probes the W-t-b vertex, provides a direct determination of Cabbibo-Kobayashi-Maskawa (CKM) matrix element $|V_{tb}|$ and offers a source of almost 100% polarized top quarks [2]. The CDF detector is described in detail in [3].

II. DATA SAMPLE & EVENT SELECTION

This analysis is based on an integrated luminosity of 3.2 fb^{-1} collected with the CDFII detector between March 2002 and August 2008. Candidate events for this analysis are selected by requiring a W + 2jets and 3jets event topology where W decays leptonically, $W \rightarrow e\nu_e$ or $W \rightarrow \mu\nu_\mu$. The data are collected with an inclusive lepton trigger that requires an electron or muon with E_T >18 GeV (P$_T$ >18 GeV/c for the muon) or missing E_T >35 GeV plus jets trigger. From this inclusive lepton dataset we select events offline with a reconstructed isolated electron E$_T$ (muon P$_T$) greater than 20 GeV, missing E_T >25 GeV and 2 jets with E$_T$ >20 GeV and $|\eta|$ <2.8. Both of the two jets should be identified as a b-jet where one jet is identified using secondary-vertex information(SecVtx) [4] and the other jet is identified using secondary-vertex(SecVtx) or impact-parameter information(JetProb) [5]. The background surviving these selection are $t\bar{t}$, W + heavy-flavorjets, i.e. $W + b\bar{b}$, $W + c\bar{c}$, $W + c$ and diboson events WW, WZ, and ZZ. Instrumental backgrounds originate from mis-tagged W+jets events (W events with light-flavor jets, i.e. with u, d, s-quark and gluon content, misidentified as heavy-flavor jets) and from non$W$ + jets events (multi-jet events where one jet is erroneously identified as a lepton).

III. BACKGROUND ESTIMATE

Estimating the background contribution after applying the event selection to the single top candidate sample is an elaborate process. NLO cross section calculations exist for diboson and $t\bar{t}$ production, thereby making the estimation of their contribution a relatively straightforward process. The main background contributions are from $W+b\bar{b}$, $W+c\bar{c}$ and $W+c$+jets, as well as mis-tagged W+ light quark jets. We determine the W+jets normalization from the data and estimate the fraction of the candidate events with heavy-flavor jets using ALPGEN Monte Carlo sample [6]. The heavy=flavor fraction were calibrated in the b-tagged W+1jet sample using data distributions which are sensitive to distinguish light-flavor from heavy-flavor jets, e.g. the mass of the secondary-vartex and, more sophisticated, the output of the Neural Network jet-flavor separator. Based on these studies, the heavy flavor content was corrected by a factor K$_{HF}$=1.44±0.4. The probability that a W + light-flavor jet is mis-tagged is parameterized using large statistics generic multi-jet data. The instrumental background contribution from non-W events are estimated using side-band data with low missing transverse energy, devoid of any signal, and we subsequently extrapolate the contribution into the signal region with large missing transverse energy, MET>25 GeV. The expected signal and background yield in the W+2jet and W+3jet sample is shown in Table I.

IV. ANALYSIS METHOD

A. Kinematics Fitter

There are two signigicant ambiguity in calculating the reconstructed M_{lnb}. One comes from the uncertainty on assigning a b-jet correctly to the b-jet from top quark decay. The other is the neutrino energy. Transverse energy of the neutorino can be measured indirectly as the missing transverse energy, but nutrino momentum z-component $P_z(\nu)$ can not be measured. The purpose of the kinematics fitter is to evaluate the neutrino momentum and find the right b-jet assignment. Neutrino momentum z-component can be caliculated as the solution in a quadratic equation using a W mass constraint and the missing transverse energy. Since we have two solutions at most, we constructed two types of likelihood-based kinematics fitter for 2 solutions case and the other case. We minimized the negative log likelihood value by varying three parameters, $P_Z(\nu Z)$, $\not\!\!E_x$ and $\not\!\!E_y$. MINUIT was used this minimization. We

CDF Run II Preliminary, L=3.2 fb^{-1}

Process	2jets	3jets
s-channel	21.5 ± 3.8	7.9 ± 1.4
t-channel	5.0 ± 0.9	6.4 ± 1.1
WW	1.8 ± 0.3	1.6 ± 0.2
WZ	7.9 ± 1.0	2.6 ± 0.3
ZZ	0.2 ± 0.0	0.1 ± 0.0
$t\bar{t}$	63.2 ± 10.9	195.5 ± 33.9
Z+jets	2.9 ± 0.6	2.1 ± 0.4
Zbb	2.7 ± 0.5	1.7 ± 0.3
Zcc	0.3 ± 0.1	0.3 ± 0.0
Wbb	143.5 ± 45.2	56.1 ± 17.6
Wcc/Wc	36.1 ± 11.3	18.1 ± 5.7
Total HF	179.6 ± 56.5	74.2 ± 23.2
Total MC	105.6 ± 15.5	218.1 ± 36.0
Mistags	32.5 ± 10.3	28.5 ± 7.9
Non-W	13.0 ± 10.4	15.0 ± 12.0
Total Prediction	330.7 ± 60.3	335.9 ± 45.2
Observed	288.0 ± 0.0	321.0 ± 0.0

TABLE I: The number of expected single top and background events in 3.2fb^{-1} of CDF data passing all event selection for all W+2b-taggaed jets.

construct a likelihood for b-jet from top decay as follows. $P_T(b)$, M_{lb}, $\cos\theta_b \times Q_{lep}$, where $P_T(b)$ is b-jet P_T, M_{lb} is an invariant mass of lepton + b-jet and $\cos\theta_b$, Q_{lep} is a scattering angle of b-jet in initial quarks ($q\bar{q}$) rest frame and Q_{lep} is a lepton charge. We pick up a b-jet which have larger likelihood as the b-jet from top decay.

B. Likelihood Function Technique

In order to discover the single top production, and to measure its rate with a highest significance, we must take advantage of as many differences between the signal and the background as possible. To this end, a variety of quantities which can be computed from the reconstructed event variables have been investigated for their ability to separate the signal from the background. As no single variable encodes any conceivable separation, a likelihood is proposed combining several variables together into one discriminant to compute the cross section limits or to discover the signal.

The Likelihood $\mathcal{L}$ is constructed first by forming the template histogram of each variable, separately for the signal and for the several backgrounds, denoted P_i^m for variable i for the background event class m and the signal. Since about 75 % of the background are W+HF and $t\bar{t}$, we used t-channel single top, W+HF and $t\bar{t}$ as the background templates. These three background classes are separately used to construct the likelihood. These histogram are normalized so that area is unity. The likelihood is defined as :

$$\mathcal{L}^{signal} = \frac{\prod_{i=1}^{n_{val}} P_i^{\text{signal}}}{\prod_{i=1}^{n_{val}} P_i^{\text{signal}} + \sum_{m=1}^{n_{bkg}} \prod_{i=1}^{n_{val}} P_i^m \times \alpha^m} \tag{1}$$

where,

$$P_i^{\text{process}} = \frac{f_i^{\text{process}}}{f_i^{\text{signal}} + \sum_{m=0}^{n_{bkg}} f_i^{\text{m}}}, \quad \alpha^m = \frac{N_{\text{eve}}^m}{\sum_{m=1}^{n_{bkg}} N_{\text{eve}}^m} \tag{2}$$

f is the bin content of template histograms of each variable, and N_{eve}^m is the number of expected events shown in table I. The likelihood ignores the correlation between the input variables, although it is critical that the predicted distributions of $\mathcal{L}$ for the signal and the backgrounds are computed using a fully correlated set of input variables - from Monte Calro or from control data sample

The figure of merit of the discriminant is $s/\sqrt{s+b}$ with the optimum parameters having the maximum value, where s is the number of signal evnets and b is the number of background events. We found the sensitivity are maximum when the following 10(9) variables are used for 2jet-bin(3jet-bin).

2jet-bin

- M_{bb} : di-jet invariant mass
- p_{Tbb} : transverse momentum for $b\bar{b}$ system
- ΔR_{bb} : transverse momentum for $b\bar{b}$ system
- $M_{l\nu b}$: invariant mass of lepton, neutorino and b-jet from top quark decay
- p_T(j1) : leading jet transverse momentum
- η(j2) : second leading jet pseudo-rapidity
- p_T(lep) : lepton transverse momentum
- $Q \times \eta$: non-b or non-top-decay assigned jet pseudo-rapidity times lepton charge.
- $\mathcal{M}_{\text{LLR}}$: Log Likelihood ratio constructed by Wbb, $t-$channel and $s-$channel matrix element.
- $\mathcal{L}_{\nu\text{sol}} \times \mathcal{L}_{bb\text{sol}}$: kinematics fitter likelihood output times the likelihood for b-jet from top decay.

3jet-bin

- ΔR_{bb} : transverse momentum for $b\bar{b}$ system
- $M_{l\nu b}$: invariant mass of lepton, neutorino and b-jet from top quark decay
- M_{invbjj} : hadronic decayed top quark invariant mass by b-jet, LF jet, and invisible jet and M_W constraint.
- p_T(non-b) : non-b assigned jet transverse momentum, if 3jet-bin.
- η(j1) : leading jet pseudo-rapidity
- η(j2) : second leading jet pseudo-rapidity
- η(lep) : lepton pseudo-rapidity
- $\cos\theta^*$: cosine angle between lepton and d-type initial quark direction at top quark restframe.
- $\mathcal{L}_{\nu\text{sol}} \times \mathcal{L}_{bb\text{sol}}$: kinematics fitter likelihood output times the likelihood for b-jet from top decay.

To maximize sensitivity we divide 8 different purity of sub sumple as follows:

- Triggered lepton, W+2jet-bin, SecVtx + SecVtx tagged
- Triggered lepton, W+2jet-bin, SecVtx + JetProb tagged
- Triggered lepton, W+3jet-bin, SecVtx + SecVtx tagged
- Triggered lepton, W+3jet-bin, SecVtx + JetProb tagged
- Untriggered muon, W+2jet-bin, SecVtx + SecVtx tagged
- Untriggered muon, W+2jet-bin, SecVtx + JetProb tagged
- Untriggered muon, W+3jet-bin, SecVtx + SecVtx tagged
- Untriggered muon, W+3jet-bin, SecVtx + JetProb tagged

V. SYSTEMATIC UNCERTAINTIES

We address systematic uncertainty from several different sources: (1)jet energy scale, (2) initial state radiation (ISR), (3) final state radiation (FSR), (4) parton distribution function, (5) the event generator, (6) the uncertainty in the event detection efficiency, (7)the uncertainty on the integrated luminosity, (8) ALPGEN Monte Carlo Factorization/Renormalization scale uncertainty, (9) uncertainty on the Monte Carlo Modeling. (10) uncertainty on the mistag model, Systematic uncertainties can influence both, the expected event yield(normalization) and the shape of the discriminant distribution. Mormalization uncertainties are estimated by calculating the variation in expected event yield due to a systematic effect. The range of systematic rate and shape variation across signal and background processes are shown in Table II. Shape uncertainties are estimated by producing shifted template histogram for each process du to the systematic effect. The bin-by-bin relative variations are used as shape systematics in the likelihood function. The letter "$\surd$" in Table II indicates that a shape systematic uncertainty has been evaluated for the particular nuisance parameter and included in the likelihood function. For all backgrounds the normalization uncertainties are represented by the uncertainty on the predicted number of background events and are incorporated in the analysis as Gaussian contributes $G(\beta|1,\Delta_j)$ in the likelihood function :

$$\mathcal{L}(\beta_1,...,\beta_5;\delta_1,...,\delta_{10}) = \prod_{k=1}^{B} \frac{e^{-\mu_k}\cdot\mu_k^{n_k}}{n_k!} \cdot \prod_{j=2}^{5} G(\beta_j|1,\Delta_j) \cdot \prod_{j=1}^{10} G(\delta_j,0,1) \tag{3}$$

$$where, \mu_k = \sum_{j=1}^{5} \beta_j \cdot \left\{ \prod_{j=1}^{12} (1+|\delta_i|\cdot(\epsilon_{ji+}H(\delta_i)+\epsilon_{ji-}H(-\delta_i))) \right\} \tag{4}$$

$$\cdot\ \alpha_{jk} \cdot \left\{ \prod_{i=1}^{12} (1+|\delta_i|\cdot(\kappa_{jik+}H(\delta_i)+\kappa_{jik-}H(-\delta_i))) \right\} \tag{5}$$

The systematic normalization and shape uncertainties are incorporated into the likelihood as nuisance parameters, conforming with a fully Bayesian treatment [7]. We take the correlation between normalization and shape uncertainties for a given source into account [8]. The relative strength of a systematic effect due to the source i is parameterized by the nuisance parameter δ_i in the likelihood function, constrained to a unit-width Gausian(last term in Equation 3). The $\pm1\sigma$ changes in the normalization of process j due to the i^{th} source of systematic uncertainty are denoted by ϵ_{ji+} and ϵ_{ji-} (see Equation part 4). The $\pm1\sigma$ changes in bin κ of discriminant templates for process j due to the i^{th} source of systematic uncertainty are quantified by κ_{jik+} and κ_{jik-} (see Equation part 5). H(δ_i) represents the Heaviside function, defined as H(δ_i)=1 for δ_i >0 and H(δ_i)=0 for δ_i <0. The Heaviside function is used to separate positive and negative systematic shifts (for which we have different normalization and shape uncertainties). The variable δ_i appears in both the term for the normalization (Equation 4) and the shape uncertinaty (Equation 5), which is how correlations between both effects are taken into account. We reduce the likelihood function to the parameter of interest (single top cross-section) by the standard Bayesian marginalizing procedure [9]

VI. RESULTS

A. Results in s-channel analysis

We analyzed to 3.2 fb^{-1} of CDF Run II Data. We predicted 29.4 events of single top s-channel signal over the 667 background events. The distributions of likelihood discriminant, which was described in Section IV B Eq. 1, are shown in Figure 1 which has two most sensitive category.

Cross Section Measurement

Figure 2(left) shows the likelihood distribution in the data with 68% region marked to show the uncertainty. The single top quark s-channel production cross section was measured to be $1.49^{+0.92}_{-0.75}$ pb. Figure 2(right) is the break down of each category, described in Section IV B. This analysis is performed under the assumption that the top quark mass is 175 GeV/c^2.

CDF RUN II Preliminary, L=3.2 fb^{-1}

Source	Rate Uncertainties for expected events	shape variation
Jet Energy Scale	4.7 %	√
Initial State Radiation	1.7 %	√
Final State Radiation	1.3 %	√
Parton Distribution Fanction	0.5 %	√
MC generator	0.5 %	
Event Selection Acceptance	1.5 %	
Integrated Luminosity	6.0 %	
Theoritical Cross Section	3.1 %	
Top Mass	2.3 %	√
Data Based Background Estimation	23 %	
Mistag Modeling		√
QCD Modeling		√
Q^2 scale in Alpgen MC		√
MC Mismodeling		√

TABLE II: Systematic uncertainties for the total prediction normalization estimated across all different processes and analysis input channels. the $\surd$ indicates that a template shape uncertainty has been evaluated for that particular nuisance parameter and has been included in the likelihood function.

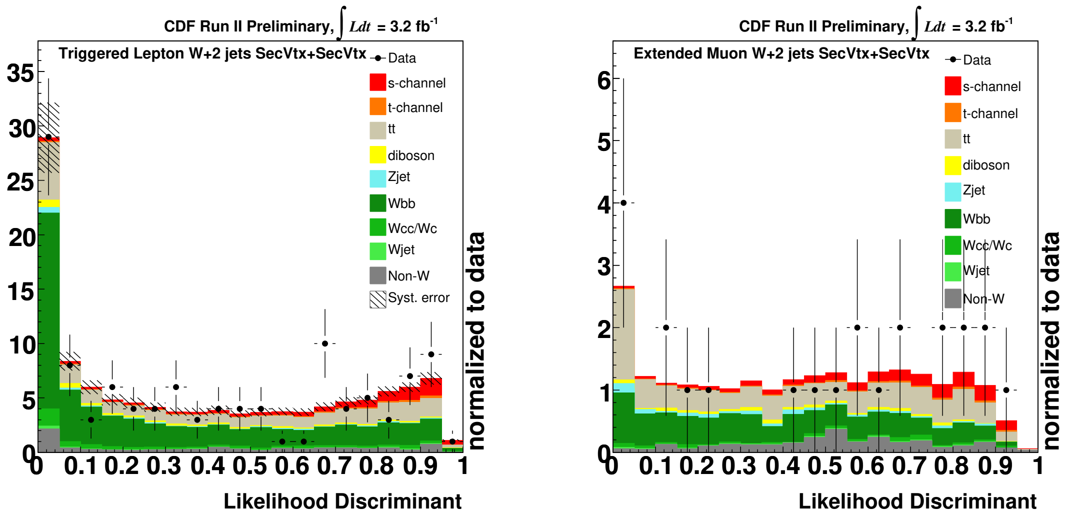

FIG. 1: Distribution of the discriminant for data and Monte Carlo. Left figure is tight lepton trigger double SecVtx category and right figure shows met+jets trigger double SecVtx category.

Measurement of $|V_{tb}|$ and Limit

The CKM matrix element $|V_{tb}|$ can be calculated very simply. Because the cross section is proportional to the square of V_{tb}, $|V_{tb}|$ is just the square root of the measured cross section divided by the expected cross section from the Standard Model as following equation.

$$|V_{tb}^{\text{measured}}|^2 = \frac{\sigma_{\text{measured}}}{\sigma_{\text{SM}}} \times |V_{tb}^{\text{SM}}|^2, \tag{6}$$

Since t-channel cross section is proportional to the $|V_{tb}|^2$ as well as s-channel, $|V_{tb}|$ is calculated from s- plus t-channel cross section from two b-tagged events, which include s-channel fraction more than 70%. This gives a result of $|V_{tb}|$=$1.32^{+0.27}_{-0.26}$(experimental) $\pm$ 0.10(theory). Because this measurement relies on the theoretical cross section of single top production, it must include the uncertainty on the cross section calculation, which is quoted here as the theoretical uncertainty.

It is also possible to set a lower limit on $|V_{tb}|$. A flat prior is assumed in $|V_{tb}|^2$, which is proportional to the measured

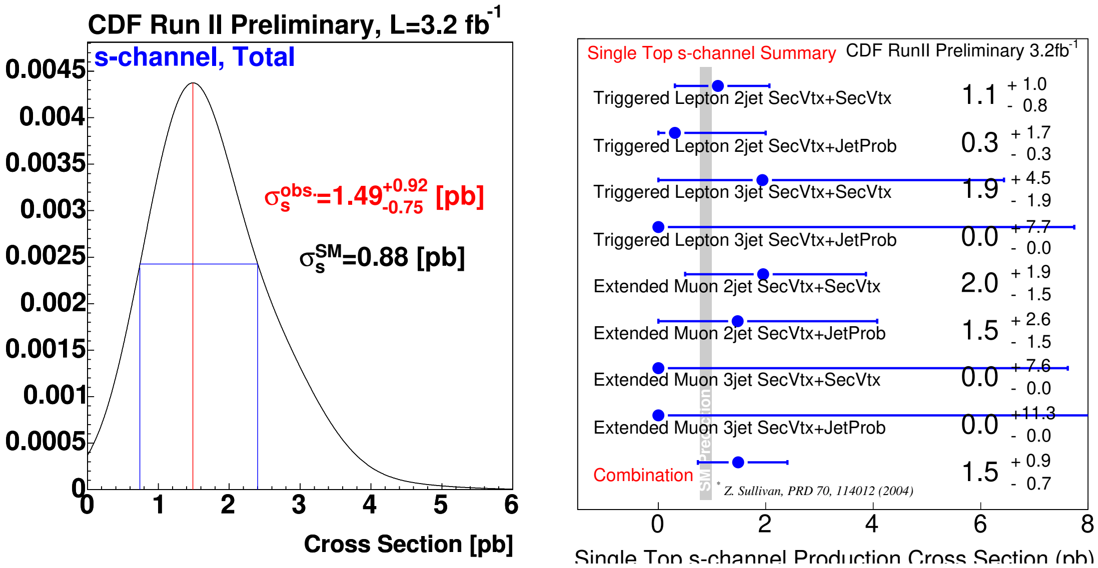

FIG. 2: Left: Cross section result using 3.2 fb$^-1$ of CDF II data. The error band shows the 68% uncertainty (all systematics included) on the measurement. Right: The break down of each category.

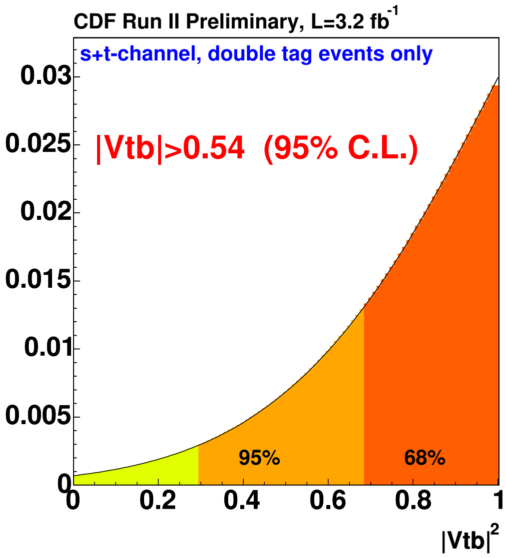

FIG. 3: The likelihood in $|V_{tb}|^2$ used to set a 95% lower limit on the value of $|V_{tb}|$.

cross section, and it is required to lie between zero and one inclusive. The likelihood must now be modified to include the systematic uncertainties on the single top production cross section and the top quark mass. This likelihood curve, shown in Figure 3, is then integrated from one, the maximum allowed value, until the area covered includes the desired percentage of the total area under the likelihood curve. Conventionally, limit are quoted at 95% C.L., so the curve is integrated until 95% of the area is included. This sets a lower limit on $|V_{tb}|$ of 0.54. Checks with pseudo-experiments show that this limit gives proper frequentist coverage.

Significance and Cross Section Upper Limit

The p-value of this measurement is obtained from the distribution of $-2\ln Q$, plotted in Figure 4(left). This measurement gives a p-value of 0.003. It is customary to interpret this probability as a number of standard deviation

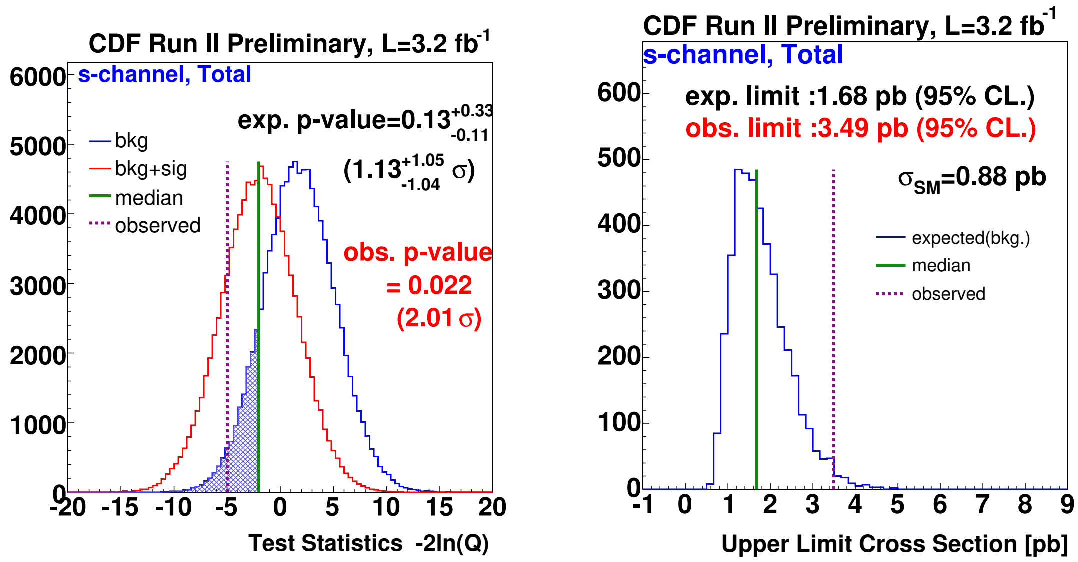

FIG. 4: (left)Distribution of the test statistics $Q = \frac{\mathcal{L}(data|s+b)}{\mathcal{L}(data|b)}$ for the singletop+background hyposhesis and the background only hypothesis in 100000 pseudo-experiments. The grean line shows the median of the sig+bkg hypothesis which is used to determine the expected p-value. Dashed purple line shows observed test statistics value which is used to determine the observed p-value.
(right)95% CL. upper limit for the s-channel single top quark production cross section.

from the mean of a Gaussian distribution, integrated from the center of distribution. In this case, the measured significance corresponds to 2.01standard deviations in Gaussian statistics.

The 95 % C.L. upper limit for the s-channel production cross section is set to $\sigma_s = 3.49$ pb assuming null signal, as shown in Figure 4(right).

B. Results in s- and t-channel analysis

We also perform t-channel optimization search with similar likelihood method discriminant, L_t, method analysis described in [11]. The final state of the single top quark t-channel production has only one b-quark typically, since b-quark jet produced by gluon splitting may be contained inside the beam pipe. On the other hand the final state of the single top quark s-channel production has two b-quark typically.

We perform s- and t-channel cross section fit simultaneously to evaluate s- and t-channel cross section separately. We used L_t discriminant described in [11] [12] for one SecVtx b-tagged category and L_s discriminant described in section IV B for double b-tagged category as following,

- triggered lepton, W+2jet, one SecVtx b-tagged sample... L_t
- triggered lepton, W+3jet, one SecVtx b-tagged sample... L_t
- triggered lepton, W+2jet, two SecVtx b-tagged sample... L_s
- triggered lepton, W+3jet, two SecVtx b-tagged sample... L_s
- extended muon, W+2jet, two SecVtx b-tagged sample ... L_s
- extended muon, W+3jet, two SecVtx b-tagged sample ... L_s
- extended muon, W+2jet, one SecVtx and one JetProb b-tagged sample ... L_s
- extended muon, W+3jet, one SecVtx and one JetProb b-tagged sample ... L_s

As a result, we obtained the likelihood fit estimate for the simultaneous s- and t-channel production cross section measurement shown in Figure 5. The cross section values are σ_s =1.41 pb and σ_t =0.98 pb with 1σ(green) and 2σ(yellow) uncertainty. The uncertainty of each production cross sections are calculated by projecting to the each axis. t-channel cross sections for this plain are linearly extraporated to the NLO calculated cross section.

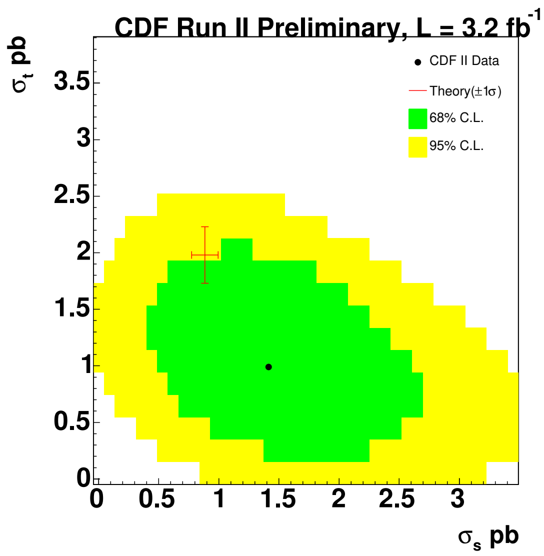

FIG. 5: The single top quark production cross section in the σ_s and σ_t plane. The best fit cross section(black dot) and it's 1σ(green) and 2σ(yellow) uncertainty. Red mark shows theoretical cross section with uncertainty. t-channel cross sections for these points are linearly extraporated to the NLO calculated cross section.

Acknowledgments

We thank the Fermilab staff and the technical staffs of the participating institutions for their vital contributions. This work was supported by the U.S. Department of Energy and National Science Foundation; the Italian Istituto Nazionale di Fisica Nucleare; the Ministry of Education, Culture, Sports, Science and Technology of Japan; the Natural Sciences and Engineering Research Council of Canada; the National Science Council of the Republic of China; the Swiss National Science Foundation; the A.P. Sloan Foundation; the Bundesministerium fuer Bildung und Forschung, Germany; the Korean Science and Engineering Foundation and the Korean Research Foundation; the Particle Physics and Astronomy Research Council and the Royal Society, UK; the Russian Foundation for Basic Research; the Comision Interministerial de Ciencia y Tecnologia, Spain; and in part by the European Community's Human Potential Programme under contract HPRN-CT-20002, Probe for New Physics.

[1] B.W.Harris *et al.*,*Phys. Rev.* D **66**, 054024 (2002).
Z.Sullivan, *Phys. Rev.* D **70**, 114012 (2004).
[2] G.Mahlon,*Phys. Rev.* D **55**, 7249 (1997), hep-ph/0011349.
[3] F. Abe, et al., Nucl. Instrum. Methods Phys. Res. A **271**, 387 (1988); D. Amidei, et al., Nucl. Instum. Methods Phys. Res. A **350**, 73 (1994); F. Abe, et al., Phys. Rev. D **52**, 4784 (1995); P. Azzi, et al., Nucl. Instrum. Methods Phys. Res. A **360**, 137 (1995); The CDFII Detector Technical Design Report, Fermilab-Pub-96/390-E
[4] D.Acosta *et al.*(CDF Collaboration),*Phys. Rev.* D **71**, 052003 (2005).
[5] D.Buskulic *et al.*(ALEPH Collaboration),*Phys. Lett.* B **313**, 535 (1993);
D.Abe *et al.*(CDF Collaboration),*Phys. Rev.* D **53**, 1051 (1996);
A.Affolder *et al.*(CDF Collaboration),*Phys. Rev.* D **64**, 032002 (2001), *Phys. Rev.* D **67**, 119901 (2003)
[6] F.Caravaglios *et al.*, M. L. Mangano *et al.*, JHEP 0307:001 (2003)
[7] L. Demortier, *Bayesian treatments of Systematic Uncertainties*, Proceeding of Advanced Statistical Techniques in Particle Physics, Grey College, Durham, 18-22 March 2002
[8] C.Ciobanu, T. Junk, T. Müller, P. Savard, B. Stelzer, W. Wagner, T. Walter, *Likelihood Function for Single Top Search with 162* pb^{-1}, CDF Note 7106 (2004)
[9] Particle Data Group, *The Review of Particle Physics*, http://pdg.lbl.gov (2004)
[10] L. Read, J.Phys G 28, 2693 (2002) and T.Junk, Nucl.Instum. Meth. 434,435(1999). See also P.Bock et al. (The LEP Collaborations), CERN-EP-98-046(1998) and CERN-EP-2000-055(2000).
[11] T. Aaltonen *et al.*, Phys. Rev. Lett. **101**, 252001 (2008).
[12] CDF Collaboration, Preliminary Result for Summer 2008 Conferences, CDF public note 9445;

CDF Collaboration, Preliminary Result for Summer 2008 Conferences, CDF public note 9451;
CDF Collaboration, Preliminary Result for Summer 2008 Conferences, CDF public note 9464;
CDF Collaboration, Preliminary Result for Summer 2008 Conferences, CDF public note 9479.